

Theoretical investigation of magnetic order in CeOFeAs

H. M. Alyahyaei and R. A. Jishi

Department of Physics, California State University, Los Angeles, California 90032

(Dated: May 23, 2022)

Density functional theory (DFT) calculations are carried out on CeOFeAs, the parent compound of the high- T_c superconductor $\text{CeO}_{1-x}\text{F}_x\text{FeAs}$, in order to determine the magnetic order of the ground state. It is found that the magnetic moments on the Fe sites adopt a collinear antiferromagnetic order, similar to the case of LaOFeAs. Within the generalized gradient approximation along with Coulomb onsite repulsion (GGA+U), we show that the Ce magnetic moments also adopt an antiferromagnetic order for which, within the CeO layer, same spin Ce sites lie along a zigzag line perpendicular to the Fe spin stripes. While within GGA the Ce 4f band crosses the Fermi level, upon inclusion of onsite Coulomb interaction the 4f band splits and moves away from the Fermi level, making CeOFeAs a Mott insulator.

I. INTRODUCTION

Recently, a new class of layered, iron-based, high temperature superconductors, has been discovered. Kamihara et al.¹ reported a superconducting transition temperature $T_c=26$ K in fluorine doped LaOFeAs. This is a member of a family of compounds known as quaternary oxypnictides with a general formula LnOMPn , where Ln is a lanthanide (La, Ce, Pr, ...), M is a transition metal (Mn, Fe, Co, ...) and Pn is a pnictogen (P, As, ...). Shortly afterwards, it was shown² that under pressure the transition temperature increased to 43 K. Hole doping, achieved by replacing trivalent La with divalent Sr gave a compound with $T_c=25$ K.³ Replacement of La by other rare earth elements gave a series of superconducting compounds $\text{ReO}_{1-x}\text{F}_x\text{FeAs}$ with Re = Ce, Pr, Nd, or Sm with transition temperatures close to or exceeding 50 K.^{4,5,6,7} Using high pressure techniques, fluorine-free but oxygen deficient samples were synthesized and found to superconduct at 55 K.⁸

The parent compound, ReOFeAs, is a layered compound consisting of a stack of alternating ReO and FeAs layers. The crystal structure is tetragonal with two molecules per unit cell. The FeAs layer consists of a square planar sheet of Fe sandwiched between two sheets of As. Upon fluorine doping these compounds become superconductors. It is not understood at this stage what mechanism lies behind superconductivity in these compounds. Understanding the electronic structure of the undoped parent compounds is necessary to understand the doped compounds, especially that in these iron-based compounds, there is an interplay between magnetism and superconductivity as is the case in the high- T_c cuprates.

Initial calculations using density functional theory (DFT) concluded that LaOFeAs is metallic and nonmagnetic but with possible antiferromagnetic (AFM) fluctuations.^{9,10,11} More extensive calculations on states with various possible magnetic orders in LaOFeAs, however, showed that the magnetic moments of the Fe ions are ordered antiferromagnetically in a stripe-like pattern in the Fe plane, resulting in a magnetic unit cell with $\sqrt{2}ax\sqrt{2}axc$ supercell structure, in contrast to the nuclear $axaxc$ unit cell.^{12,13,14,15} Indeed, neutron scattering

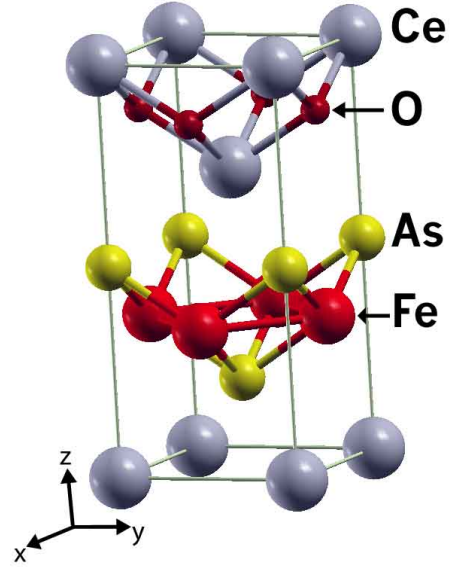


FIG. 1: (color online) The unit cell of CeOFeAs.

measurements on LaOFeAs reveal the existence of such a collinear AFM state at temperatures below 137 K.¹⁶

In this work we study the electronic structure of the parent compound CeOFeAs using DFT within the generalized gradient approximation (GGA). We consider various possible magnetic orders of the Fe and Ce ions. We show that in the ground state the magnetic moments of the Fe ions adopt a collinear AFM order as in the case of LaOFeAs. Within GGA, the Ce sites are paramagnetic, but when the onsite Coulomb interaction is taken into account (GGA+U), the magnetic moments at the Ce sites, resulting from the 4f electrons, also adopt an AFM order with a zigzag-like pattern.

II. METHOD

The first-principles calculations presented in this work were performed using the all-electron full potential linear augmented plane wave plus local orbitals (FP-

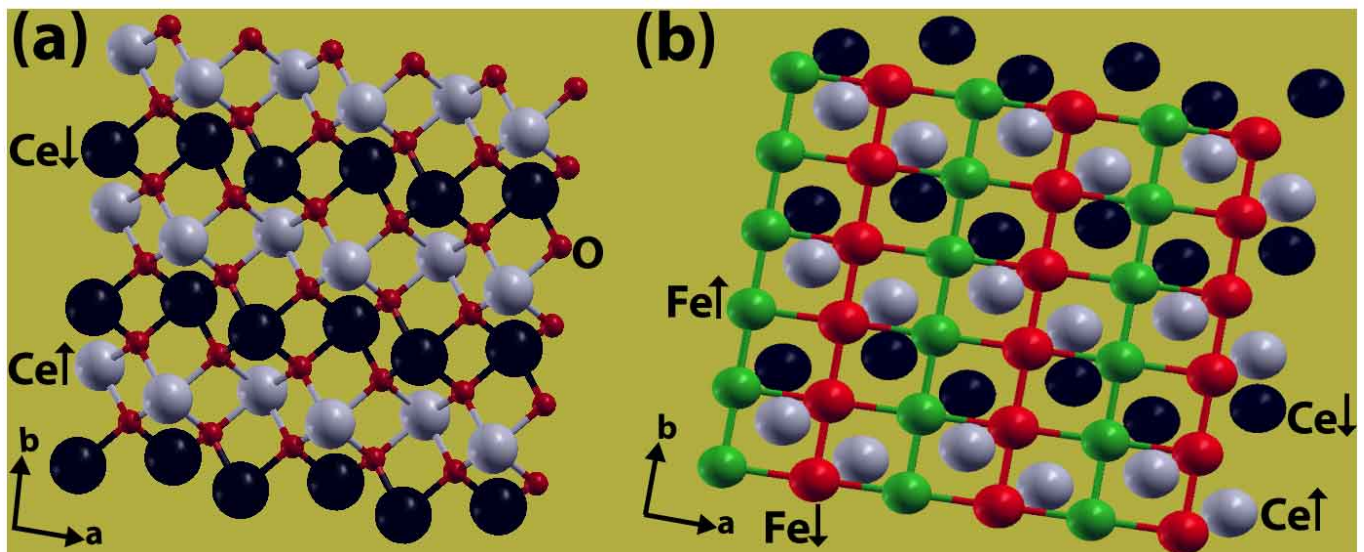


FIG. 2: (color online) The {Fe: c-AFM; Ce: z-a-AFM} magnetic phase of CeOFeAs. In (a), a single CeO layer is shown. The gray balls represent spin-up Ce ions while the black ones represent spin-down Ce ions. The spin-up Ce ions (as well as the spin-down Ce ions) run along a zigzag chain parallel to the a -axis. In (b) we show a different perspective of the same magnetic phase. Here we show only the Fe and Ce ions. The Fe spin stripes are along the b -direction while the Ce spin stripes are "wrinkled" to become zigzag chains along the a -direction.

LAPW+lo) method as implemented in WIEN2K code¹⁷. In this method the core states are treated in a fully relativistic way but the valence states are treated at a scalar relativistic level. The exchange-correlation potential was calculated using the generalized gradient approximation (GGA) as proposed by Pedrew, Burke, and Ernzerhof (PBE)¹⁸.

For calculations in this work, the nuclear unit cell is tetragonal, with lattice constants $a = b = 3.998 \text{ \AA}$, $c = 8.652 \text{ \AA}$. The atomic positions within the unit cell were given by Chen et al.⁷. The nuclear unit cell, shown in Fig. 1, has 8 atoms. For the magnetic phase in which the magnetic moments of the Fe ions adopt a collinear AFM, the magnetic unit cell is a $\sqrt{2}ax\sqrt{2}axc$ supercell of the original nuclear cell, and it contains 16 atoms. In this magnetic unit cell, $a = 5.654 \text{ \AA}$, $c = 3.998 \text{ \AA}$, and the a and b axes are rotated by 45° in the $a - b$ plane with respect to the a and b axes of the nuclear unit cell. In the magnetic unit cell, the crystal coordinates of the 4 Ce atoms are: Ce1 (0, 0, 0), Ce2 (0.5, 0.0, z), Ce3 (0, 0.5, z), and Ce4 (0.5, 0.5, 0), where $z = 0.71692$. Ce1 and Ce4 belong to a Ce-plane above the O-plane, while Ce2 and Ce3 belong to a Ce-plane below the O-plane. These two Ce-planes along with the O-plane sandwiched between them constitute the CeO layer. The radii of the muffin-tin spheres for Ce, O, Fe, and As atoms were taken to be $2.33a_0$, $2.07a_0$, $2.38a_0$, and $2.11a_0$ respectively, where a_0 is the Bohr radius. These radii are chosen so that the nearby muffin-tin spheres are almost touching. For all structures considered in this work we set the parameter $R_{\text{MT}}K_{\text{MAX}}=7$, where R_{MT} is the smallest muffin-tin radius and K_{MAX} is a cutoff wave-vector. The valence

wavefunctions inside the muffin-tin spheres are expanded in terms of spherical harmonics up to $l_{\text{max}} = 10$ while in the interstitial region they are expanded in plane waves with a wave-vector cutoff K_{MAX} , and the charge density is Fourier expanded up to $G_{\text{MAX}}=13a_0^{-1}$. Convergence of the self consistent field calculations is attained with a strict charge convergence tolerance of 0.00001 e.

III. RESULTS AND DISCUSSION

To begin with, we consider within GGA, various magnetic orders of the Fe magnetic moments in the Fe plane: nonmagnetic, ferromagnetic (FM), antiferromagnetic (AFM), and collinear antiferromagnetic (c-AFM). We find that the collinear antiferromagnetic order of the Fe magnetic moments has the lowest energy, regardless of the spin order on the Ce sites. The energy of the collinear antiferromagnetic order of the Fe moments is lower than the antiferromagnetic order by 0.031 eV per Fe atom, lower than the FM order by 0.156 eV per Fe atom, and lower than the nonmagnetic phase by 0.146 eV per Fe atom. In the AFM order, every spin-up Fe site is surrounded by 4 nearest neighbor (NN) spin-down Fe sites, whereas in the c-AFM order, among the 4 NN Fe sites surrounding a spin-up Fe site, two are spin-up and the other two are spin-down, but the 4 next nearest neighbor (NNN) Fe sites are all spin-down. The AFM and the c-AFM orders within the Fe plane were described elsewhere^{12,13,14,15,16} in connection with LaOFeAs. That the Fe magnetic moments, in the Fe-plane, adopt the c-AFM order in CeOFeAs is consistent with what has already

TABLE I: The relative energies per Ce ion in five different magnetic orders of the Ce ions in CeOFeAs. In all these phases, the paramagnetic (PM), ferromagnetic (FM), antiferromagnetic (AFM), zigzag-along-a antiferromagnetic (z-a-AFM), and zigzag-along-b antiferromagnetic (z-b-AFM), the magnetic order refers only to the magnetic moments on the Ce sites. In all these phases, the magnetic moments of the Fe ions are ordered in a collinear antiferromagnetic (c-AFM) fashion with Fe spin stripes in the Fe-plane taken to be parallel to the b -axis. The zero of energy corresponds to the case where the Ce ion is nonmagnetic. Here $U' = U - J$, where U is the onsite Coulomb interaction and J is the exchange coupling.

Phase \rightarrow Method \downarrow	Energy (eV / Ce)				
	PM	FM	AFM	z-a-AFM	z-b-AFM
GGA	-0.179	-0.030	-0.043	-0.037	-0.037
GGA+U, $U' = 2.5$ eV	-0.176	-0.437	-0.438	-0.472	-0.449
GGA+U, $U' = 5.0$ eV	-0.176	-0.446	-0.486	-0.531	-0.487

been found in LaOFeAs^{12,13,14,15,16}.

In the remaining calculations we fix the spin order within the Fe-plane to be c-AFM, with the Fe spin stripes taken to be along the b -direction in the magnetic unit cell. A spin-up stripe in the $a - b$ plane is a line of Fe ions, parallel to the b -axis, with up-spins; this is surrounded in the $a - b$ plane by two spin-down stripes, also parallel to the b -axis. Fixing the spin order in the Fe-plane, we now focus our attention on the spin order of the Ce ions. Considering only the Ce sites in CeOFeAs, we note that every Ce site (for example, Ce1) has 4 NN Ce sites at a distance of 3.74 Å (2 Ce2 and 2 Ce3 sites) and 4 NNN Ce sites at a distance of 3.998 Å (4 Ce4 sites). Thus for the magnetic order on the Ce sites we consider six different cases:

1) The nonmagnetic (NM) phase, where the magnetic moment on every Ce site is constrained to be zero.

2) The paramagnetic (PM) phase, where the magnetic moment on each Ce site is non zero, but the spins on different Ce sites are not correlated.

3) The ferromagnetic (FM) order, where the magnetic moments on all Ce sites are aligned in the same direction.

4) The antiferromagnetic order (AFM), where every spin-up Ce site has 4 NN spin-down Ce sites. Here, the four Ce ions in the magnetic unit cell, Ce1-Ce2-Ce3-Ce4, have the spin arrangement uddu, where u stands for up and d stands for down. In this phase, considering a CeO layer (one O-plane surrounded by two Ce-planes) the Ce spins in one plane are all up, while the Ce spins in the other plane are all down. That is, in each Ce-plane the order is ferromagnetic (FM), but the magnetization in one Ce-plane is opposite to that in the nearby Ce-plane lying across from the O-plane.

5) The zigzag antiferromagnetic (z-a-AFM) order where a spin-up Ce site has 2 NN spin-up Ce sites, 2 NN spin-down Ce sites, and 4 NNN spin-down Ce sites. The four Ce ions in the unit magnetic cell, Ce1-Ce2-Ce3-Ce4, have the spin arrangement uudd. Here, if we connect the same-spin NN Ce ions in a given CeO layer, we obtain a zigzag chain running parallel to the a -axis direction, as shown in Fig. 2. In this phase, if we consider a single Ce-plane (for example, the one containing Ce1 and Ce4), then it is clear that the Ce magnetic moments in

this plane adopt a simple AFM order where each spin-up Ce ion (for example Ce1) is surrounded by 4 spin-down Ce ions (4 Ce4 ions). So in each of the two Ce-planes surrounding the O-plane in the CeO layer, the magnetic order is AFM in such a way as to produce same-spin zigzag chains running along the a -direction.

6) The zigzag antiferromagnetic (z-b-AFM) order for which the four Ce ions in the unit magnetic cell, Ce1-Ce2-Ce3-Ce4, have the spin arrangement udud. This is similar to case 5 except that the same-spin Ce ions lie on zigzag chains running along the b -direction. In an isolated CeO layer, this phase will have the same energy as phase 5, but since the Fe-plane has spin stripes along the b -axis, it follows that these two phases will not be degenerate if there is an interaction between the Fe spins and the Ce spins.

We make the following two remarks about how the calculations are performed :

i) It is not really possible to calculate directly the total energy of the paramagnetic (PM) phase, because in this phase the magnetic moments on the Ce sites are randomly oriented; it follows that a unit cell in the (PM) phase will contain a very large number of Ce atoms. On the other hand, the average magnetic moment per Ce site is zero in the PM phase. Therefore, one way to calculate the total energy of the PM phase is to constrain the magnetic moment on every Ce site to be zero; this will make the total energy of the PM phase coincide with that of the nonmagnetic (NM) phase, which is not the case in reality. To get the around this problem, we note that in the high temperature γ -phase of elemental Cerium crystal, The NN distance between Ce atoms is 3.65 Å¹⁹ and that in this phase, while the 6s and 5d valence electrons are itinerant, the 4f electron is localized on the Ce site, giving rise to a localized magnetic moment. In CeOFeAs, The distance between the NN Ce sites is 3.74 Å, slightly larger than in γ -phase Ce; hence we expect that here the 4f electrons are strongly localized on the Ce sites, giving rise to magnetic moments localized on these sites. We calculate the total energy of an isolated Ce⁺³ ion for both cases when the ion is nonmagnetic (half the 4f¹ electron is spin-up, the other half is spin-down) and when it

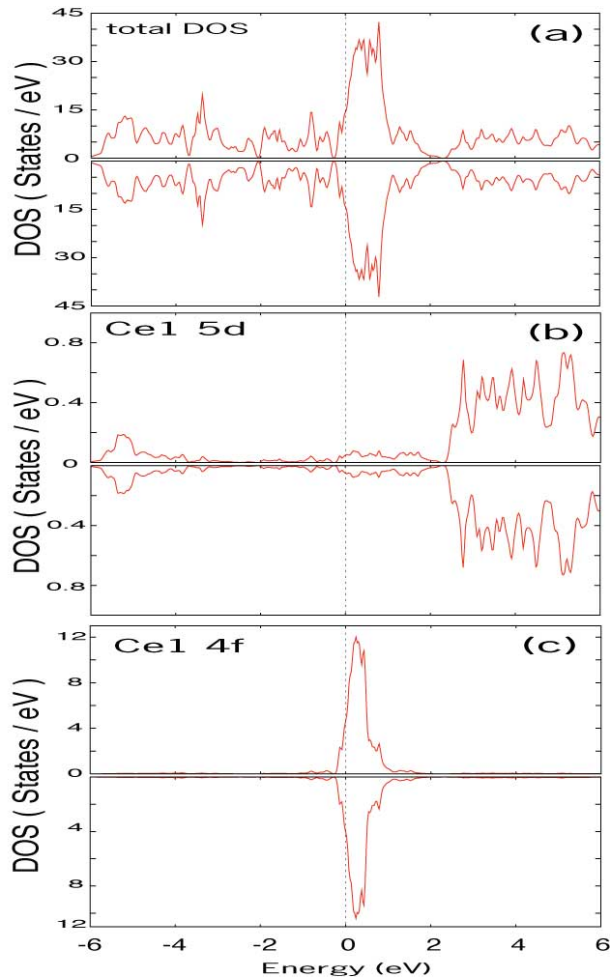


FIG. 3: (color online) spin-resolved density of state (DOS) in CeOFeAs in the {Fe: *c*-AFM; Ce: *z*-*a*-AFM} phase, within GGA. The upper half of each panel displays the spin-up DOS, while the lower half displays the spin-down DOS. In (a) the total DOS is shown, while (b) and (c) show the partial DOS due to the Ce1 5d and 4f states, respectively.

is magnetic. We find that the energy difference is

$$E_{\text{magnetic}}(\text{Ce}^{+3}) - E_{\text{nonmagnetic}}(\text{Ce}^{+3}) = -0.176 \text{ eV}.$$

Therefore, we make the reasonable assumption that -0.176 eV/Ce ion approximates the energy difference between the energies of CeOFeAs in the PM phase (Fe ions have *c*-AFM order but Ce ions are paramagnetic) and in the NM phase (Fe ions have *c*-AFM order while Ce ions are nonmagnetic).

ii) In doing the GGA+*U* calculations, we need the value of *U*-*J*, where *U* is the onsite Coulomb repulsion and *J* is the exchange coupling. For Fe, $J \simeq 0.9 \text{ eV}$, and *U* has an empirical value in the range 3.5-5.1 eV²⁰; in our calculation we take *U*-*J*= 3.4 eV for the Fe ions. For the Ce ions values for *U*-*J* ranging from 2 – 5 eV for GGA calculations are found in the literature,^{21,22,23} though the value *U*-*J*= 5 eV appears to give better results in describing the electronic structure of cerium oxides. In the

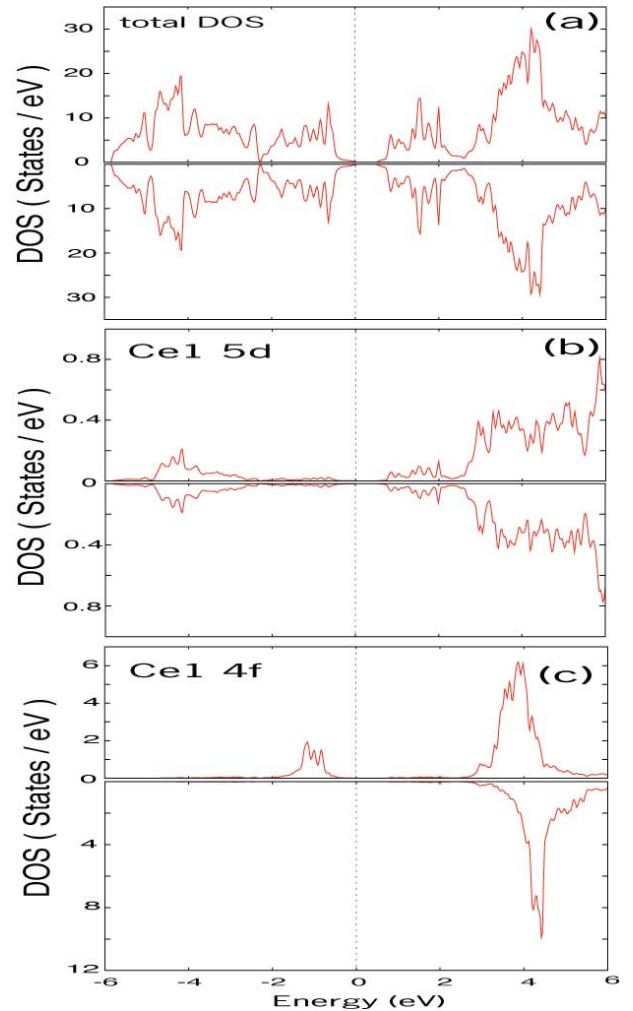


FIG. 4: (color online) spin-resolved density of state (DOS) in CeOFeAs in the {Fe: *c*-AFM; Ce: *z*-*a*-AFM} phase, within GGA+*U* with *U*-*J*=5 eV. The upper half of each panel displays the spin-up DOS, while the lower half displays the spin-down DOS. In (a) the total DOS is shown, while (b) and (c) show the partial DOS due to the Ce1 5d and 4f states, respectively.

calculations reported here we consider two cases where *U*-*J* is taken to be 2.5 eV or 5 eV.

A summary of the total energy calculation is given in Table I, where we report the differences in the total energy among the six cases listed earlier. We take the energy of the NM phase, in which the Fe moments adopt *c*-AFM order and the Ce ions are nonmagnetic, as our zero energy. The results in Table I show that within GGA, in the absence of the onsite Coulomb interaction, the ground state of CeOFeAs is one where the Fe magnetic moments adopt *c*-AFM order while the Ce sites are paramagnetic. In the presence of onsite Coulomb interaction, on the other hand, the Fe magnetic moments adopt *c*-AFM order and the Ce magnetic moments *z*-*a*-AFM order. Our results are consistent with the low temperature specific heat measurements⁷ which show, besides a phase

transition at 145 K, associated with the magnetic ordering of the Fe magnetic moments, a new antiferromagnetic transition occurring at 3.7 K. Since no such transition is observed in LaOFeAs¹⁴, this transition in CeOFeAs is attributed to an antiferromagnetic ordering of the Ce magnetic moments. Within GGA+U calculation, due to the proximity of the energy values of the different magnetic orders of the Ce magnetic moments, and the existence of some disorder, which tends to reduce the energy difference between the various phases, these magnetic orders compete, rendering the Ce sites paramagnetic. At very low temperatures, the phase {Fe: c-AFM; Ce: z-a-AFM} in which Fe spins have c-AFM order and Ce spins z-a-AFM order, being the lowest in energy, will prevail. The spin order in this phase is shown in Fig. 2.

The electronic density of state (DOS) in CeOFeAs in the phase {Fe: c-AFM; Ce: z-a-AFM} is shown in Figs. 3 and 4 as calculated within GGA and GGA+U, respectively. Note that the GGA calculation (Fig. 3) produces a wide Ce 5d-band and a narrow Ce 4f band both crossing the Fermi level; the DOS at the Fermi energy is dominated by 4f states, making CeOFeAs a metal. With on-site Coulomb interaction taken into account, CeOFeAs becomes a Mott insulator. Fig. 4 shows that within GGA+U, apart from the wide Ce 5d-bands, the Ce 4f band is split into the 4f⁰ and 4f² bands. Photoemission experiments should reveal the positions of these bands, providing a check on the validity of the results obtained in these calculations.

IV. CONCLUSIONS

In conclusion, the DFT calculations indicate that the Fe magnetic moments in CeOFeAs adopt a collinear antiferromagnetic order, similar to that in LaOFeAs. Whereas the La ion in LaOFeAs is nonmagnetic, the Ce ion in CeOFeAs carries a magnetic moment due to its localized 4f electron. Within GGA+U, we show that the Ce magnetic moments also adopt an antiferromagnetic order similar to that adopted by the Fe ions. However, while the Fe ions in the FeAs layer all lie on one plane, giving rise to a collinear AFM order, the Ce ions in the CeO layer lie on two different planes surrounding the oxygen ions plane. In each Ce plane, a Ce ion is surrounded by 4 NNN Ce ions that have spins opposite to the spin of the central ion. Viewed in this light, we can say that in the ground state, within each Ce plane, the spin order is simply antiferromagnetic, where each spin-up site is surrounded by 4 spin-down sites in the same plane. However, for a given spin-up Ce ion on a given Ce plane, its 4 NN Ce ions all lie on the other Ce plane of the CeO layer; of those 4 NN Ce ions, two will be spin-up and two will be spin-down. If we connect each spin-up Ce site to its NN spin-up sites within a given CeO layer, we will end up with a zigzag chain running perpendicular to the Fe spin stripes in the Fe-plane. A similar zigzag chain is obtained if we connect NN spin-down Ce sites within any one CeO layer.

-
- ¹ Y. Kamihara, T. Watanabe, M. Hirano, and H. Hosono, *J. Am. Chem. Soc.* **130**, 3296 (2008).
- ² H. Takahashi, K. Igawa, K. Arii, Y. Kamihara, M. Hirano, and H. Hosono, *Nature* **453**, 376 (2008).
- ³ H. H. Wen, G. Mu, L. Fang, H. Yang, and X. Y. Zhu, *Europhys. Lett.* **82**, 17009 (2008).
- ⁴ D. A. Zocco, J. J. Hamlin, R. E. Baumbach, M. B. Maple, M. A. McGuire, A. S. Sefat, B. C. Sales, R. Jin, D. Mandrus, J. R. Jeffries, S. T. Weir, and Y. K. Vohra, *arXiv:Cond-mat* **0805.4372** (2008).
- ⁵ Z. A. Ren et al., *arXiv:Cond-mat* **0803.4283** (2008).
- ⁶ X. H. Chen et al., *Nature* **453**, 761 (2008).
- ⁷ X. H. Chen et al., *arXiv:Cond-mat* **0803.3790** (2008).
- ⁸ Z. A. Ren et al., *arXiv:Cond-mat* **0804.2582** (2008).
- ⁹ H. Eschrig, *arXiv:Cond-mat* **0804.0186** (2008).
- ¹⁰ G. Xu et al., *arXiv:Cond-mat* **0804.1282** (2008).
- ¹¹ K. Haule et al., *arXiv:Cond-mat* **0803.1279** (2008).
- ¹² S. Ishibashi, K. Terakura, and H. Hosono, *J. Phys. Soc. Japan* **77**, 053709 (2008).
- ¹³ T. Yildirim, *Phys. Rev. Lett.* **101**, 057010 (2008).
- ¹⁴ J. Dong et al., *arXiv:Cond-mat* **0803.3426** (2008).
- ¹⁵ F. Ma et al., *arXiv:Cond-mat* **0803.3370** (2008).
- ¹⁶ C. de la Cruz et al., *Nature* **453**, 899(2008).
- ¹⁷ P. Blaha, K. Schwarz, G. K. H. Madsen, D. Kvasnicka, and J. Luitz, *WIEN2K, an augmented plane wave + local orbitals program for calculating crystal properties* (Techn. Universität, Wien, Austria, 2001), ISBN 3-9501031-1-2.
- ¹⁸ J. P. Perdew, K. Burke, and M. Ernzerhof, *Phys. Rev. Lett.* **77**, 3865 (1996).
- ¹⁹ D. C. Koskenmaki, and K. A. Gschneidner, Jr., *Handbook on the physics and chemistry of rare earths: Metal*, edited by K. A. Gschneidner, Jr. and L. Eyring, (North Holland physics publishing, Amsterdam, 1981, vol 1, chap.4).
- ²⁰ V. I. Anisimov, J. Zaanen, and O. K. Andersen, *Phys. Rev. B* **44**, 943(1991).
- ²¹ M. Cococcioni, and S. de Gironcoli, *Phys. Rev. B* **71**, 035105(2005).
- ²² D. A. Anderson, S. I. Simak, B. Johansson, I. A. Abrikosov, and N. V. Skorodumova, *Phys. Rev. B* **75**, 035109 (2007).
- ²³ C. Loschen, J. Carrasco, K. M. Neyman, and F. Illas, *Phys. Rev. B* **75**, 035118 (2007).